Chemical Science

ROYAL SOCIETY OF CHEMISTRY

EDGE ARTICLE

View Article Online
View Journal | View Issue

Cite this: *Chem. Sci.*, 2024, **15**, 10448

All publication charges for this article have been paid for by the Royal Society of Chemistry

Controlling rates and reversibilities of elimination reactions of hydroxybenzylammoniums by tuning dearomatization energies†

Zihuan Fu, ‡ Joseph W. Treacy, ‡ Brock M. Hosier, K. N. Houk * and Heather D. Maynard *

Hydroxybenzylammonium compounds can undergo a reversible 1,4- or 1,6-elimination to afford quinone methide intermediates after release of the amine. These molecules are useful for the reversible conjugation of payloads to amines. We hypothesized that aromaticity could be used to alter the rate of reversibility as a distinct thermodynamic driving force. We describe the use of density functional theory (DFT) calculations to determine the effect of aromaticity on the rate of release of the amine from hydroxybenzylammonium compounds. Namely, the aromatic scaffold affects the dearomatization reaction to reduce the kinetic barrier and prevent the reversibility of the amine elimination. We consequently synthesized a small library of polycyclic hydroxybenzylammoniums, which resulted in a range of release half-lives from 18 minutes to 350 hours. The novel mechanistic insight provided herein significantly expands the range of release rates amenable to hydroxybenzylammonium-containing compounds. This work provides another way to affect the rate of payload release in hydroxybenzylammoniums.

Received 7th May 2024
Accepted 23rd May 2024

DOI: 10.1039/d4sc02985b

rsc.li/chemical-science

Introduction

Cleavage reactions that release amine-containing payloads either spontaneously or upon an external trigger are of great interest. The most common strategies for this include elimination from fluorenylmethoxycarbamate (Fmoc) and benzyl carbamate linkages. The Fmoc cleavage is entirely mediated by pH and undergoes a β-elimination reaction to release amine-containing payloads.[1] The hydroxy- or amino-benzyl carbamate linkage can proceed through either a 1,4- or 1,6-elimination. These carbamate linkers leverage the irreversible release of carbon dioxide as the main thermodynamic driving force (Fig. 1a).[2,3] Other chemistries such as various enzyme-cleavable linkages[4,5] and cyclization-driven linkers[6] have also been explored to release amines.

Recently, we developed a class of hydroxybenzylammonium-based traceless linkers for conjugating polymers onto proteins' lysine residues or N-terminus with tunable rates of release.[7] These hydroxybenzylammoniums released the payloads with tunable half-lives from 20 hours to 144 hours depending on the electron-donating group incorporated onto the aromatic ring. Using key mechanistic insight gained from density functional theory (DFT) calculations, we discovered that the loss of amine payload and formation of the quinone methide intermediate was a reversible step in this reaction. Therefore, an intramolecular nucleophilic agent was designed *in silico* to subvert the entropic cost of an intermolecular reaction by interacting with the quinone methide intermediate, preventing the reversibility of the reaction (Fig. 1b). The addition of the pendant nucleophilic group accelerated the half-life by five-fold and achieved a reaction half-life of 5.5 hours and a first-order rate constant of 3.53×10^{-5} s^{-1}. However, certain applications with self-immolative linkers may necessitate even faster release of the payload. Accessing these higher rates would require a different approach from the use of electron donating substituents and pendant nucleophilic groups.

Inspired by work showing the increased rates of azaquinone methide-mediated release of benzylic phenols when polycyclic aromatic cores were used (Fig. 1c),[8–12] we hypothesized that leveraging aromaticity as a thermodynamic driving force would serve as a separate approach to modulate the release rates of the hydroxybenzylammoniums (Fig. 1d). Using experimental and computational mechanistic studies, we were able to elucidate the key role of aromaticity in the release of amines. This mechanistic insight led us to develop hydroxybenzylammoniums with amine release half-lives from 18 minutes to 350 hours.

Results and discussion

DFT calculations

To examine the effect of aromatic rings on the release, we initially computed the free energy diagrams for the 1,4-benzene

Department of Chemistry and Biochemistry, California NanoSystems Institute, University of California, Los Angeles, California, 90095-1569, USA. E-mail: maynard@chem.ucla.edu

† Electronic supplementary information (ESI) available. See DOI: https://doi.org/10.1039/d4sc02985b

‡ Z. F. and J. W. T. contributed equally to this work.

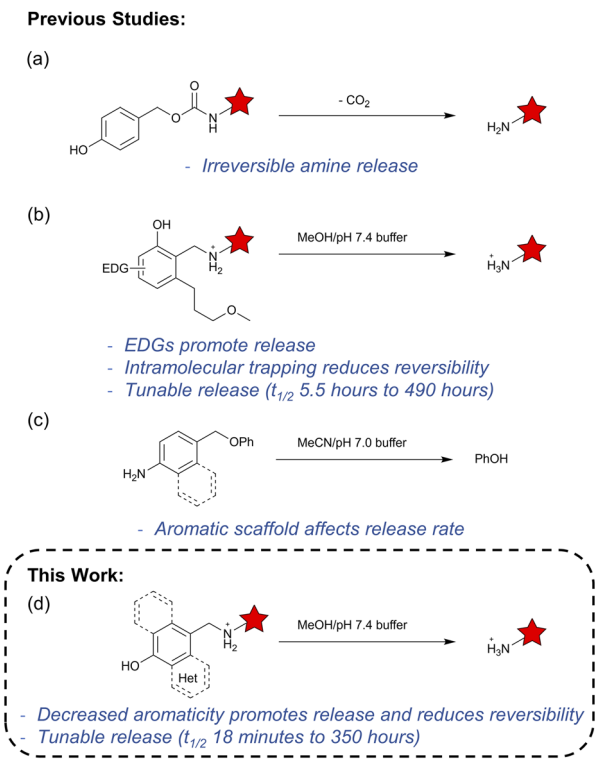

Fig. 1 (a) Benzyl carbamates for amine release. (b) Hydroxybenzylammoniums with electron-donating groups and intramolecular trapping arms.[7] (c) Polycyclic azaquinone methide-mediated release of benzylic phenols.[8] (d) Polycyclic aromatic hydroxybenzylammoniums. Star indicates a potential payload of interest (fluorophore, polymer, protein/peptide, *etc.*).

substrate at the M06-2X/aug-cc-pVTZ, CPCM(Water)//B3LYP-D3/6-31+G(d,p), CPCM(Water) level of theory using methylamine as a model amine (Fig. 2a). Previously, we have noted that the release of these hydroxybenzylammoniums is pH-dependent,[7] but in this instance, the pK_a of the phenol proton should not be significantly affected by the addition of more aromatic rings (See ESI Fig. S48†).[13] As the initial deprotonation event should have a similar Gibbs free energy (ΔG) (*ca.* +2.5 kcal mol^{-1}) for the substrates, we have computed the reaction starting from the zwitterionic species *Int1*. *Int1* then undergoes the elimination of methylamine with a Gibbs activation free energy ($\Delta G^{\ddagger}$) of 14.0 kcal mol^{-1}. However, the formation of the quinone methide *Int2* is endergonic by 0.4 kcal mol^{-1}, indicating the reversibility of this reaction. Examining the 1,4-naphthalene substrate, we observe a $\Delta G^{\ddagger}$ of 12.0 kcal mol^{-1} with a ΔG_{Rxn} of −4.5 kcal mol^{-1}, which has a lower $\Delta G^{\ddagger}$ and ΔG_{Rxn} compared to the 1,4-benzene substrate. These results indicate that the amine release for the 1,4-naphthalene scaffold should be both faster and less reversible than the 1,4-benzene substrate. Fusion of additional benzene rings may further affect the amine release rate, so we computed the 1,4-anthracene and 1,4-tetracene substrates, which lead to $\Delta G^{\ddagger}$ of 10.8 and 11.1 kcal mol^{-1} and ΔG_{Rxn} of −6.6 and −7.1 kcal mol^{-1}, respectively. Comparing the substrates' free energy diagrams (Fig. 2a), we observe an Evans-Polanyi type relationship wherein the ΔG_{Rxn} is proportional to the $\Delta G^{\ddagger}$. Additionally, we observe a noticeable decrease in the C–N bond distance when comparing the transition state geometries (Fig. 2b), emphasizing the earlier transition state for the more conjugated substrates.

We also sought to examine how hydroxybenzylammonium substitution in the polyaromatic system affects the reaction energetics. Examining the 9,10-anthracene and 5,12-tetracene substrates, we observe $\Delta G^{\ddagger}$ of 8.5 and 7.4 kcal mol^{-1} and ΔG_{Rxn} of −11.9 and −14.3 kcal mol^{-1}, respectively. These substrates provide a pronounced $\Delta\Delta G^{\ddagger}$ compared to their distally substituted counterparts. By examining the Polansky Aromaticity Index, a measure of the local aromaticity in polyaromatic hydrocarbons, of the parent hydrocarbon scaffold, we observe a trend wherein the less aromatic systems have a lower $\Delta G^{\ddagger}$ (Fig. 2c), indicating that the dearomatization reaction is more facile for these substrates. Since the central rings are less aromatic compared to the distal rings, the $\Delta G^{\ddagger}$ for these substrates is significantly lowered (*i.e.* 9,10-anthracene *vs.* 1,4-anthracene and 5,12-tetracene *vs.* 1,4-tetracene). Based on our computational results, we proposed that the 6,13-pentacene substrate would have the most favorable $\Delta G^{\ddagger}$ and ΔG_{Rxn} as it has the lowest Polansky Aromaticity Index among the computed substrates.[14,15] We computed the free energy diagram for this substrate and observed a $\Delta G^{\ddagger}$ of 6.5 kcal mol^{-1} and ΔG_{Rxn} of −16.8 kcal mol^{-1} (Fig. 2a), which is in agreement with our hypothesis. From these seven substrates, we can elucidate the effect that aromatic ring fusion and location of the hydroxybenzylammonium play in this reaction. Namely, these two factors facilitate the dearomatization reaction, which leads to a decrease in $\Delta G^{\ddagger}$ and a decrease in reversibility for the amine elimination.

Synthesis of hydroxybenzylammonium scaffolds

To validate these computational predictions, we sought to synthesize all of the computed substrates (Fig. 2a). Using commercially available 4-hydroxybenzaldehyde and 4-hydroxy-1-naphthaldehyde, phenethylamine conjugates **1** and **2a** were prepared *via* reductive amination, respectively. To synthesize the 1,4-anthracene scaffold, we performed a Sandmeyer reaction with the commercially available 1-amino-4-hydroxyanthraquinone using copper(II) bromide and *tert*-butyl nitrite, forming bromoanthraquinone **4**. This was then methylated (**5**) and subsequently reduced with sodium borohydride to yield 1-bromo-4-methoxyanthracene (**6**). Lastly, a sequence of demethylation (**7**) followed by lithiation and formylation with DMF afforded the hydroxyaldehyde **8** (Scheme 1, see ESI for details†). **8** was then conjugated to phenethylamine *via* reductive amination to form **3a**.

Difficulty in regioselective functionalization to form the 1,4-tetracene, 5,12-tetracene, and 6,13-pentacene substrates precludes their synthesis. Additionally, computational examination of the 1,4-anthracene and 9,10-anthracene hydroxyaldehyde tautomers indicated that the 9,10-anthracene favors tautomerization to the anthrone, whereas the 1,4-anthracene prefers the hydroxyaldehyde scaffold (See ESI pages S87 and 88†).[16] Formation of the anthrone likely prevents formation of the corresponding hydroxybenzylammonium after reductive

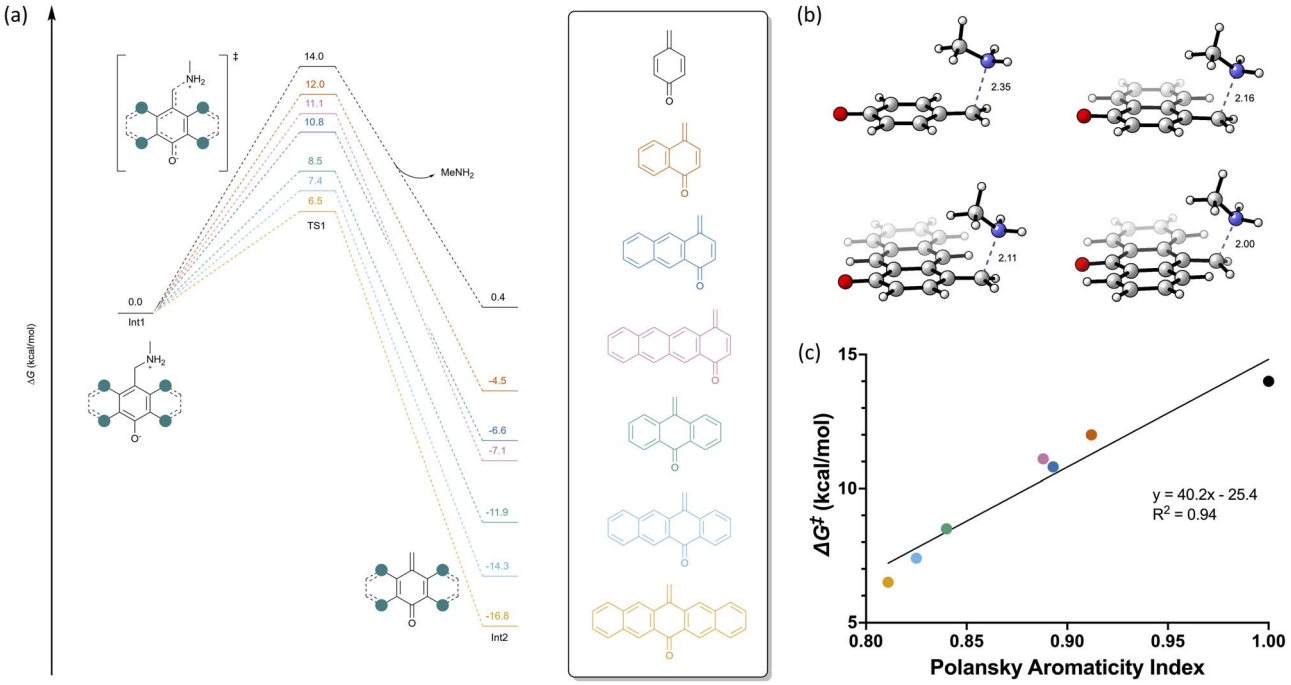

Fig. 2 (a) Free energy diagrams for polycyclic aromatic hydroxybenzylammonium release calculated at the M06-2X/aug-cc-pVTZ, CPCM(Water)//B3LYP-D3/6-31+G(d,p), CPCM(Water) level of theory. (b) *TS1* geometries calculated for 1,4-benzene, 1,4-naphthalene, 1,4-anthracene, and 9,10-anthracene-based hydroxybenzylammoniums. (c) Calculated free energy of activation at the aforementioned level of theory plotted against the corresponding Polansky Aromaticity Index of the parent hydrocarbon scaffold.

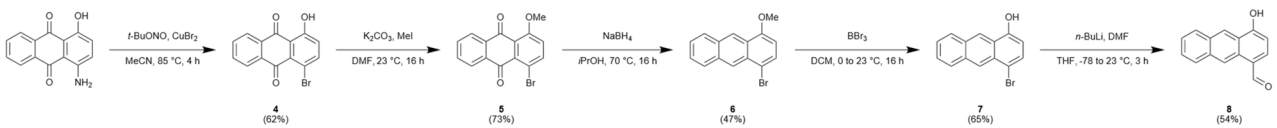

Scheme 1 Synthesis of 1,4-anthracene hydroxybenzaldehyde **8**.

amination, so we shifted our focus to the release studies of the 1,4-benzene, 1,4-naphthalene, and the 1,4-anthracene scaffolds that prefer the hydroxyaldehyde tautomer.

Release studies of polycyclic aromatic hydroxybenzylammoniums

Phenethylamine was chosen as a model amine payload for high-performance liquid chromatography (HPLC) kinetic analysis. The release studies were performed using standard conditions with 5 mM solution of the hydroxybenzylammonium in a 1 : 1 mixture of methanol and 0.1 M Tris buffer at pH 7.4, where the appearance of phenethylamine was monitored *via* HPLC and quantified using the area under the curve at 254 nm. As we previously demonstrated, the 1,4-hydroxybenzylammonium (**1**) shows no release, likely due to the reversibility of the quinone methide formation. We next sought to experimentally profile the release of the 1,4-naphthalene-based hydroxybenzylammonium. **2a** has a release half-life of six hours and first-order rate constant of 2.98×10^{-5} s^{-1} (Fig. 3), which approaches the fastest rate constant from our initial report (3.53×10^{-5} s^{-1}) and was synthesized in one step from commercially available starting materials. This finding also validates our computational prediction that we are able to modulate the release rate by tuning the aromatic scaffold of the hydroxybenzylammonium.

With DFT calculations showing that the 1,4-anthracene substrate has a $\Delta\Delta G^{\ddagger}$ of -1.2 kcal mol^{-1} and a $\Delta\Delta G_{Rxn}$ of -2.1 kcal mol^{-1} compared to the 1,4-naphthalene scaffold (Fig. 2a), we profiled the release for the 1,4-anthracene substrate. Due to its diminished solubility in 1 : 1 methanol and Tris buffer, the release assays for **3a** were performed at 1 mM concentration instead of the standard 5 mM. In agreement with DFT calculations, the more conjugated 1,4-anthracene system (**3a**) showed a 20-fold increase in release rate compared to naphthalene **2a**, pushing the release half-life to 18 minutes and rate constant to 6.12×10^{-4} s^{-1} (Fig. 3).

To ensure that both the naphthalene **2a** and anthracene **3a** proceed though our proposed mechanism of deprotonation and quinone methide formation, we prepared methylated derivatives **2b** and **3b** (See ESI for details†). As expected, this prevented the deprotonation of the phenol and subsequent formation of the quinone methide intermediate, leading to no observed release of phenethylamine (Fig. 3).

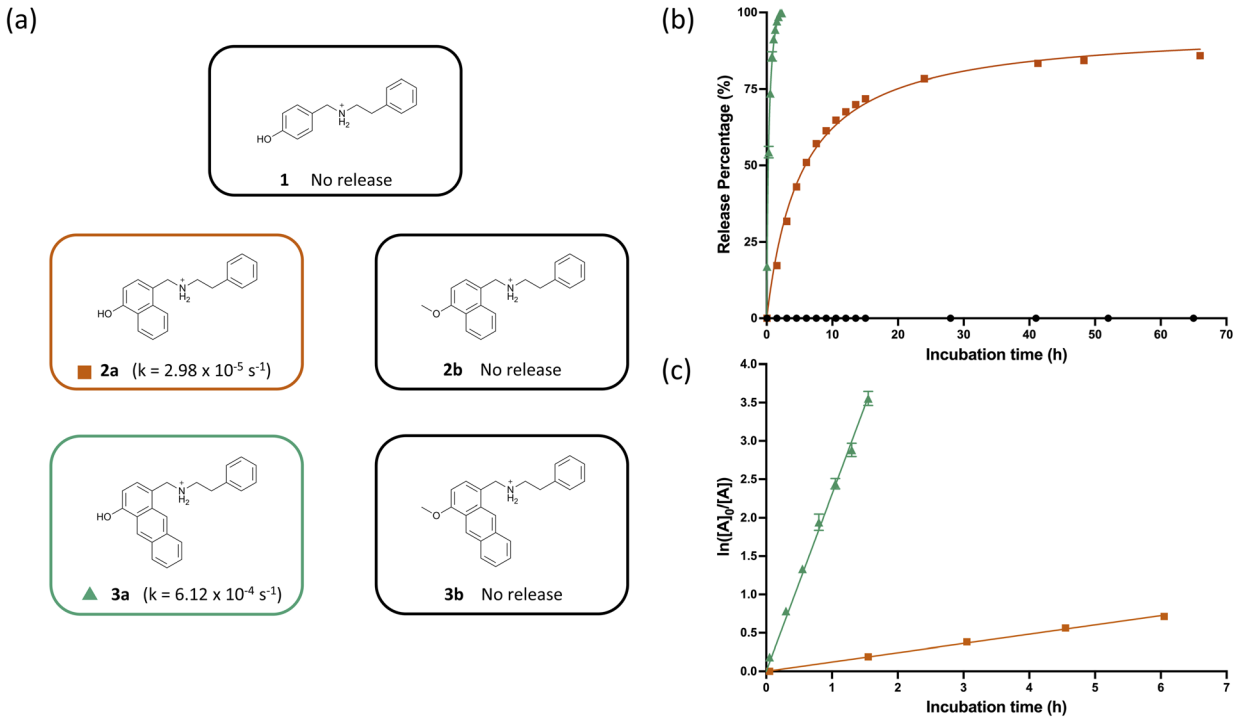

Fig. 3 (a) Library of polycyclic aromatic–phenethylamine conjugates prepared and their experimentally determined release rate constants. (b) Phenethylamine release kinetics of **1**, **2a**, and **3a** ($n = 3$, some error bars are smaller than markers) carried out at 5 mM of the benzene- or naphthalene-hydroxybenzylammoniums or 1 mM of the anthracene-hydroxybenzylammonium in a 1 : 1 mixture of methanol and 0.1 M Tris buffer (pH 7.4). (c) First-order plot of phenethylamine release kinetics of **2a** and **3a** ($n = 3$, some error bars are smaller than markers).

Heteroaromatic hydroxybenzylammonium and azabenzylammonium release

Previous literature reports demonstrate that in the case of benzyl carbamate-based self-immolative linker release, the pyridine core system releases faster than its benzene analog.[17] This is likely due to the lower pK_a of the phenol proton in the heteroaromatic case, so we also hypothesized that this may aid in the release rate in the hydroxybenzylammoniums (See ESI Fig. S49†). Therefore, we decided to explore the effect of heteroaromatic cores on the rate of release in our hydroxybenzylammoniums (Fig. 4).

Since 5-hydroxypicolinaldehyde is the only stable isomer of hydroxypyridine,[18] we first prepared its phenethylamine conjugate **9** *via* reductive amination. However, subjecting it to standard release conditions did not show any release, similar to the benzene core (**1**).

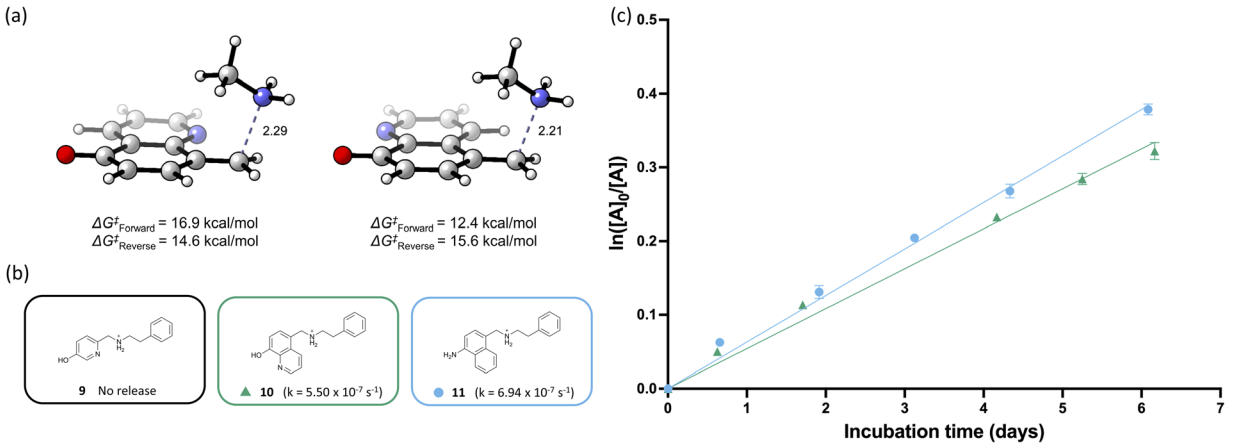

Fig. 4 (a) *TS1* structures calculated at the B3LYP-D3/6-31+G(d,p), CPCM(water) level of theory for 5- and 8-hydroxyquinoline benzylammoniums and calculated free energies of activation for the forward and reverse reactions at the M06-2X/aug-cc-pVTZ, CPCM(Water)//B3LYP-D3/6-31+G(d,p), CPCM(Water) level of theory. (b) Library of pyridine-, quinoline-, and azanaphthalene-based phenethylamine conjugates synthesized and their experimentally determined release rate constants. (c) First-order plot of phenethylamine release kinetics ($n = 3$, some error bars are smaller than markers) carried out at 5 mM of the hydroxy- or azabenzylammonium in a 1 : 1 mixture of methanol and 0.1 M Tris buffer (pH 7.4).

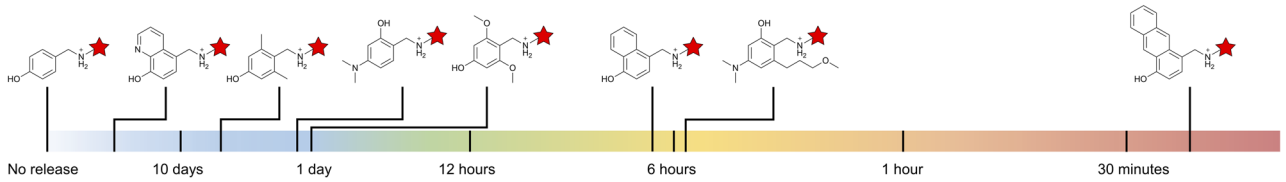

Fig. 5 Release half-life spectrum of hydroxybenzylammonium molecules. Release half-lives displayed are from this report as well as our previous article.[7]

We then shifted our focus to a quinoline core system, positing that the additional conjugation would accelerate the release. Two isomers of quinolines could be prepared that undergo the 1,6-elimination, so we first sought to computationally examine the 5- and 8-hydroxyquinoline isomers to determine an optimal experimental candidate. The 5-hydroxyquinoline substrate has a $\Delta\Delta G^{\ddagger}$ of +4.5 kcal mol^{-1} compared to the 8-hydroxyquinoline substrate, likely due to the hydrogen bonding of the benzylammonium N–H protons to the nitrogen atom in the quinoline that is disrupted during the dearomatization reaction (Fig. 4a, see ESI for details†).

Accordingly, the 8-hydroxyquinoline substrate was synthesized (See ESI for details†) and reductive amination with phenethylamine was performed to generate **10** for further release assays. The release assay was carried out using the standard protocol, and the 8-hydroxyquinoline benzylammonium **10** exhibited a rate constant of 5.50×10^{-7} s^{-1} with a half-life of 350 hours, which is significantly slower compared to the naphthalene scaffold **2a** (Fig. 4b and c). We hypothesize that despite the lower pK_a of the phenol proton, the heteroaromatic rings are more electron deficient, which leads to slower release of the amine-based payload.

Lastly, we examined different elimination triggers to determine how the azaquinone methide elimination compared to its quinone methide counterpart. A Boc-protected amino-naphthylamine was prepared and deprotection with TFA prior to the release assay afforded the azaquinone methide-based benzylammonium **11**. However, it showed a significant decrease in rate (half-life of 277 hours and rate constant of 6.94×10^{-7} s^{-1}) compared to the quinone methide benzylammonium **2a** (Fig. 4b and c). This is likely due to the reduced donating capability of the aniline ($\sigma_p = -0.66$) compared to the phenoxide ($\sigma_p = -0.81$).[19]

We believe that further elaboration and incorporation of these hydroxybenzylammonium motifs into peptide- and protein–polymer conjugates would allow for additional rate tuning of these materials as traceless, self-immolative linkers. The expanded half-lives presented in this study (>10 days to <30 minutes, Fig. 5) give users the option to choose an aromatic scaffold amenable to their desired application. Incorporation of a cleavable phenol protecting group would allow for a stimuli-responsive release, which could provide temporal control over payload release from the hydroxybenzylammonium scaffold. Additionally, we propose that this strategy is also amenable to the release of secondary and tertiary amines (See ESI pages S85 and 86†), though the tertiary amine would necessitate formation of the hydroxybenzylammonium *via* a substitution reaction instead of reductive amination.

Conclusions

The hydroxybenzylammonium elimination reaction can provide scientists with a useful tool for reversible modification of compounds as a self-immolative linker. In prodrugs and antibody-drug conjugates, self-immolative linkers are often used to temporarily inactivate the therapeutics to limit off-target effects. However, when they are exposed to the requisite stimuli, the self-immolative linkers are cleaved, releasing the active payload.[20,21] These linkers have also been explored as a useful strategy to employ in formulations of polymer–protein conjugates. Polymer conjugation is widely employed to address some of the challenges for these therapeutics, such as instability in the presence of internal and external stressors and short circulation times.[22–27] However, conjugation of large polymers onto the surface of the proteins often significantly reduces the bioactivity of the proteins.[28–32] Therefore, the use of self-immolative linkers between the protein and polymer, where the covalent linker cleaves upon external stimuli, allows the native proteins to be released, reversing the loss of activity by removing the conjugated polymer.[33] Additionally, self-immolative monomers have been incorporated into stimuli-responsive materials that are designed to undergo a cascade and sequential depolymerization upon the removal of the end-capping group.[34–36]

Using DFT calculations, we uncovered the effect that polycyclic aromatic cores have on accelerating the release of an amine-containing payload from the hydroxybenzylammoniums. The release of the amine is accelerated in the polycyclic aromatic substrates due to the reduced aromaticity in these systems which simultaneously prevents the reversibility of the elimination. We subsequently prepared a series of polycyclic aromatic-based hydroxybenzylammoniums and were able to achieve half-lives as fast as 18 minutes. Lastly, we examined the effect of heteroaromatic hydroxybenzylammonium and azabenzylammonium scaffolds on the release of amines, but they did not show improved rates of release. Thus, these results demonstrate another avenue to tune the release profile of the hydroxybenzylammoniums and the computational and experimental synergy available in this field.

Data availability

All data are available free of charge in the ESI,† including experimental details, NMR spectra, characterization, and coordinates of computed structures.

Author contributions

Zihuan Fu: conceptualization, synthesis, formal analysis, writing – original draft. Joseph W. Treacy: conceptualization, computation, formal analysis, writing – original draft. Brock M. Hosier: synthesis, formal analysis. K. N. Houk: supervision, writing – review and editing, funding acquisition. Heather D. Maynard: conceptualization, supervision, writing – review and editing, funding acquisition. All authors have given approval to the final version of the manuscript.

Conflicts of interest

The authors declare no conflict of interest.

Acknowledgements

This work was funded in part by the NSF (CHE-2003946) and NIH (R01DK127908). Z. F. thanks National Institute of Health Chemistry–Biology Interface Training Grant (T32GM136614) for support. J. W. T. thanks UCLA Dissertation Year Fellowship for support. B. M. H. thanks UCLA Ramsey Summer Fellowship for support. This work used computational and storage services associated with the Hoffman2 Shared Cluster provided by the UCLA Institute for Digital Research and Education's Research Technology Group. NMR spectrometers are supported by the National Science Foundation under equipment grant no. CHE-1048804 and the S10 program of the NIH Office of Research Infrastructure Programs, under grant S10OD028644.

Notes and references

1 T. Peleg-Shulman, H. Tsubery, M. Mironchik, M. Fridkin, G. Schreiber and Y. Shechter, Reversible PEGylation: A Novel Technology To Release Native Interferon α2 over a Prolonged Time Period, *J. Med. Chem.*, 2004, **47**, 4897–4904.
2 R. Erez and D. Shabat, The azaquinone-methide elimination: comparison study of 1,6- and 1,4-eliminations under physiological conditions, *Org. Biomol. Chem.*, 2008, **6**, 2669–2672.
3 S. Lee, R. B. Greenwald, J. McGuire, K. Yang and C. Shi, Drug Delivery Systems Employing 1,6-Elimination: Releasable Poly(ethylene glycol) Conjugates of Proteins, *Bioconjugate Chem.*, 2001, **12**, 163–169.
4 G. M. Dubowchik and R. A. Firestone, Cathepsin B-sensitive dipeptide prodrugs. 1. A model study of structural requirements for efficient release of doxorubicin, *Bioorg. Med. Chem. Lett.*, 1998, **8**, 3341–3346.
5 G. M. Dubowchik, K. Mosure, J. O. Knipe and R. A. Firestone, Cathepsin B-sensitive dipeptide prodrugs. 2. Models of anticancer drugs paclitaxel (Taxol®), mitomycin C and doxorubicin, *Bioorg. Med. Chem. Lett.*, 1998, **8**, 3347–3352.
6 S. Huvelle, A. Alouane, T. L. Saux, L. Jullien and F. Schmidt, Syntheses and kinetic studies of cyclisation-based self-immolative spacers, *Org. Biomol. Chem.*, 2017, **15**, 3435–3443.
7 D. A. Rose, J. W. Treacy, Z. J. Yang, J. H. Ko, K. N. Houk and H. D. Maynard, Self-Immolative Hydroxybenzylamine Linkers for Traceless Protein Modification, *J. Am. Chem. Soc.*, 2022, **144**, 6050–6058.
8 J. S. Robbins, K. M. Schmid and S. T. Phillips, Effects of Electronics, Aromaticity, and Solvent Polarity on the Rate of Azaquinone–Methide-Mediated Depolymerization of Aromatic Carbamate Oligomers, *J. Org. Chem.*, 2013, **78**, 3159–3169.
9 K. M. Schmid and S. T. Phillips, Effect of aromaticity on the rate of azaquinone methide-mediated release of benzylic phenols, *J. Phys. Org. Chem.*, 2013, **26**, 608–610.
10 A. Alouane, R. Labruère, T. Le Saux, F. Schmidt and L. Jullien, Self-Immolative Spacers: Kinetic Aspects, Structure–Property Relationships, and Applications, *Angew. Chem., Int. Ed.*, 2015, **54**, 7492–7509.
11 H. Kim, A. D. Brooks, A. M. DiLauro and S. T. Phillips, Poly(carboxypyrrole)s That Depolymerize from Head to Tail in the Solid State in Response to Specific Applied Signals, *J. Am. Chem. Soc.*, 2020, **142**, 9447–9452.
12 J. Xu, C. Lv, Q. Shi, J. Zhang, N. Wang, G. Zhang, J. Hu and S. Liu, Controlled Self-Assembly of Discrete Amphiphilic Oligourethanes with a Cascade Self-Immolative Motif, *Angew. Chem., Int. Ed.*, 2023, **62**, e202306119.
13 X. Pan, H. Wang, C. Li, J. Z. H. Zhang and C. Ji, MolGpka: A Web Server for Small Molecule pKa Prediction Using a Graph-Convolutional Neural Network, *J. Chem. Inf. Model.*, 2021, **61**, 3159–3165.
14 P. Bultinck, R. Ponec, A. Gallegos, S. Fias, S. V. Damme and R. Carbó-Dorca, Generalized Polansky Index as an Aromaticity Measure in Polycyclic Aromatic Hydrocarbons, *Croat. Chem. Acta*, 2006, **79**, 363–371.
15 M. Randić, Aromaticity of Polycyclic Conjugated Hydrocarbons, *Chem. Rev.*, 2003, **103**, 3449–3606.
16 B. Ośmiałowski, E. D. Raczyńska and T. M. Krygowski, Tautomeric Equilibria and Pi Electron Delocalization for Some MonohydroxyarenesQuantum Chemical Studies, *J. Org. Chem.*, 2006, **71**, 3727–3736.
17 R. Perry-Feigenbaum, P. S. Baran and D. Shabat, The pyridinone-methide elimination, *Org. Biomol. Chem.*, 2009, **7**, 4825–4828.
18 J. Frank and A. R. Katritzky, Tautomeric pyridines. Part XV. Pyridone–hydroxypyridine equilibria in solvents of differing polarity, *J. Chem. Soc., Perkin Trans. 2*, 1976, 1428–1431.
19 C. Hansch, A. Leo and R. W. Taft, A survey of Hammett substituent constants and resonance and field parameters, *Chem. Rev.*, 1991, **91**, 165–195.
20 V. V. S. R. Edupuganti, J. D. A. Tyndall and A. B. Gamble, Self-immolative Linkers in Prodrugs and Antibody Drug Conjugates in Cancer Treatment, *Recent Pat. Anti-Cancer Drug Discov.*, 2021, **16**, 479–497.
21 P. L. Carl, P. K. Chakravarty and J. A. Katzenellenbogen, A novel connector linkage applicable in prodrug design, *J. Med. Chem.*, 1981, **24**, 479–480.
22 S. B. Gunnoo and A. Madder, Bioconjugation – using selective chemistry to enhance the properties of proteins

and peptides as therapeutics and carriers, *Org. Biomol. Chem.*, 2016, **14**, 8002–8013.

23 E. M. Pelegri-O'Day, E.-W. Lin and H. D. Maynard, Therapeutic Protein–Polymer Conjugates: Advancing Beyond PEGylation, *J. Am. Chem. Soc.*, 2014, **136**, 14323–14332.

24 C. Yang, D. Lu and Z. Liu, How PEGylation Enhances the Stability and Potency of Insulin: A Molecular Dynamics Simulation, *Biochemistry*, 2011, **50**, 2585–2593.

25 P. B. Lawrence and J. L. Price, How PEGylation influences protein conformational stability, *Curr. Opin. Chem. Biol.*, 2016, **34**, 88–94.

26 J. M. Harris and R. B. Chess, Effect of pegylation on pharmaceuticals, *Nat. Rev. Drug Discovery*, 2003, **2**, 214–221.

27 V. Gupta, S. Bhavanasi, M. Quadir, K. Singh, G. Ghosh, K. Vasamreddy, A. Ghosh, T. J. Siahaan, S. Banerjee and S. K. Banerjee, Protein PEGylation for cancer therapy: bench to bedside, *J. Cell Commun. Signaling*, 2019, **13**, 173.

28 J. Morgenstern, G. Gil Alvaradejo, N. Bluthardt, A. Beloqui, G. Delaittre and J. Hubbuch, Impact of Polymer Bioconjugation on Protein Stability and Activity Investigated with Discrete Conjugates: Alternatives to PEGylation, *Biomacromolecules*, 2018, **19**, 4250–4262.

29 C. S. Fishburn, The Pharmacology of PEGylation: Balancing PD with PK to Generate Novel Therapeutics, *J. Pharm. Sci.*, 2008, **97**, 4167–4183.

30 M. Lucius, R. Falatach, C. McGlone, K. Makaroff, A. Danielson, C. Williams, J. C. Nix, D. Konkolewicz, R. C. Page and J. A. Berberich, Investigating the Impact of Polymer Functional Groups on the Stability and Activity of Lysozyme–Polymer Conjugates, *Biomacromolecules*, 2016, **17**, 1123–1134.

31 B. S. Tucker, J. D. Stewart, J. I. Aguirre, L. S. Holliday, C. A. Figg, J. G. Messer and B. S. Sumerlin, Role of Polymer Architecture on the Activity of Polymer–Protein Conjugates for the Treatment of Accelerated Bone Loss Disorders, *Biomacromolecules*, 2015, **16**, 2374–2381.

32 A. Abuchowski, J. R. McCoy, N. C. Palczuk, T. van Es and F. F. Davis, Effect of covalent attachment of polyethylene glycol on immunogenicity and circulating life of bovine liver catalase, *J. Biol. Chem.*, 1977, **252**, 3582–3586.

33 Y. Gong, J.-C. Leroux and M. A. Gauthier, Releasable Conjugation of Polymers to Proteins, *Bioconjugate Chem.*, 2015, **26**, 1172–1181.

34 Y. Xiao, X. Tan, Z. Li and K. Zhang, Self-immolative polymers in biomedicine, *J. Mater. Chem. B*, 2020, **8**, 6697–6709.

35 A. Sagi, R. Weinstain, N. Karton and D. Shabat, Self-Immolative Polymers, *J. Am. Chem. Soc.*, 2008, **130**, 5434–5435.

36 O. Shelef, S. Gnaim and D. Shabat, Self-Immolative Polymers: An Emerging Class of Degradable Materials with Distinct Disassembly Profiles, *J. Am. Chem. Soc.*, 2021, **143**, 21177–21188.